Nonaxisymmetric Local Magnetostatic Equilibrium

J. Candy and E.A. Belli

General Atomics, P.O. Box 85608, San Diego, CA 92186-5608, USA

Abstract

In this work we outline an approach to the problem of local equilibrium in non-axisymmetric configurations that adheres closely to Miller's original method for axisymmetric plasmas [R.L. Miller, et al., Phys. Plasmas **5**, 973 (1998)]. We also describe a spectral method for solution of the resulting partial differential equations. We verify the correctness of the spectral method, in the axisymmetric limit, through comparisons with an independent numerical solution. Some analytic results for the two-dimensional case are given, and the connection to Boozer coordinates is clarified.

Email address: `candy@fusion.gat.com` (J. Candy and E.A. Belli)

1. Introduction

The local equilibrium method [1, 2, 3] is a powerful tool for providing metric coefficients required to evaluate the differential operators that appear in axisymmetric neoclassical, gyrokinetic, and MHD ballooning stability calculations. This approach ensures consistency with the equations of magnetostatic equilibrium (i.e., the Grad-Shafranov equation in the axisymmetric case). The approach suggested by Miller [4] is particularly useful insofar as one can specify not only the shape of the flux surface, but also the rates of change of the shape (for example, the Shafranov shift dR_0/dr, or the rate of change of elongation, $d\kappa/dr$) which are required for the solution of the gyrokinetic equations, for instance. Although Miller's original formulation used nine parameters to characterize the equilibrium, this has been generalized to an arbitrary number of shape parameters to achieve any desired accuracy [5]. Unlike a global equilibrium solver, the Miller approach allows for fast, systematic shaping studies on plasma transport and stability.

An analytical approach to the generalization of the local equilibrium method to three-dimensional configurations was described some time ago by Hegna [6]. The approach is elegant and maintains a strong connection to the underlying differential geometry. However, how to adapt the magnetic differential equations derived in that work to suit a Miller-type workflow is not discussed. Methods for numerical solution are also not discussed. The goal of the present work is to describe an alternative approach for the 3D problem that generalizes Miller's original one, and to develop a spectral method for solution of the resulting nonlinear partial differential equations. The resulting formalism should be suitable for neoclassical [7, 8], gyrokinetic [9, 10], and MHD ballooning [11] calculations in nonaxisymmetric geometry.

The distinction between the present approach and that in Ref. [6] is discussed by Boozer [12]. According to Boozer's characterization of the problem, in addition to the shape, there is a function $f_s(\bar{\theta}, \bar{\varphi})$ that must be specified. In the present work, that choice is $f_s(\bar{\theta}, \bar{\varphi}) = J_s(\bar{\theta}, \bar{\varphi})$, where J_s is a suitably normalized Jacobian. In Hegna's work, the choice is $f_s(\bar{\theta}, \bar{\varphi}) = \bar{\theta} - \theta$, where $\bar{\theta}$ is an arbitrary poloidal angle (the parametric angle in this work) and θ is the magnetic poloidal angle (the straight fieldline angle in this work).

The outline of the paper is as follows. In Sec. 2, we derive the general form of the equations for magnetostatic equilibrium. In Sec. 3, the Mercier-Luc expansion technique is generalized to nonaxisymmetric flux-surface shape. The zeroth and first order equations describing local equilibria are derived in Secs 4 and 5, respectively. And finally, in Sec. 6, we show how to write selected differential operators in terms of computed quantities.

2. Equations of magnetostatic equilibrium

2.1. Magnetic field representation and tensor identities

We are concerned only with the case in which there are good magnetic surfaces, in which case the magnetic field can be written as

$$\mathbf{B} = \nabla z^1 \times \nabla \left(z^2 - \iota z^3 \right) = \frac{1}{\sqrt{g}} \left(\frac{\partial \mathbf{x}}{\partial z^3} + \iota \frac{\partial \mathbf{x}}{\partial z^2} \right) \tag{1}$$

where $(z^1, z^2, z^3) \doteq (\chi, \theta, \varphi)$ are nonorthogonal toroidal coordinates with Jacobian

$$\sqrt{g} = \frac{\partial \mathbf{x}}{\partial z^1} \cdot \frac{\partial \mathbf{x}}{\partial z^2} \times \frac{\partial \mathbf{x}}{\partial z^3} = \frac{1}{\nabla z^1 \cdot \nabla z^2 \times \nabla z^3} \ . \tag{2}$$

In this representation, χ is the toroidal flux over 2π, whereas θ and φ are straight fieldline angles in the poloidal and toroidal directions. The rotation transform is given by $\iota = 1/q = d\chi/d\psi$, where q is the safety factor and ψ is the poloidal flux over 2π. Here, we note the transformation relations between the reciprocal basis:

$$\nabla z^j = \sum_i g^{ij} \frac{\partial \mathbf{x}}{\partial z^i} \quad \leftrightarrow \quad \frac{\partial \mathbf{x}}{\partial z^j} = \sum_i g_{ij} \nabla z^i \tag{3}$$

where ∇z^i and $\partial \mathbf{x}/\partial z^i$ are the contravariant and covariant vectors, respectively. In addition, we note the relation

$$\frac{\partial \mathbf{x}}{\partial z^i} = \sqrt{g}\, \nabla z^j \times \nabla z^k \quad \text{with} \quad \{ijk\} = \{123\}, \{231\}, \{312\} \tag{4}$$

which implies the important orthogonality relation

$$\nabla z^i \cdot \frac{\partial \mathbf{x}}{\partial z^j} = \sum_k g^{ki} g_{kj} = \delta^i_j \ . \tag{5}$$

Finally, the elements of the covariant and contravariant metric tensors are

$$g_{ij} \doteq \frac{\partial \mathbf{x}}{\partial z^i} \cdot \frac{\partial \mathbf{x}}{\partial z^j} \quad \text{and} \quad g^{ij} \doteq \nabla z^i \cdot \nabla z^j \ . \tag{6}$$

In what follows we will express all results in terms of the g_{ij}. In Appendix A, we outline the connection between the present coordinates and Boozer coordinates.

2.2. Nonorthogonal, nonaxisymmetric equilibrium formulation

Momentum balance together with Ampère's law determine the basic equations of nonrotating magnetostatic equilibrium

$$\mathbf{J} \times \mathbf{B} = c\, \nabla p \ , \tag{7}$$

$$\nabla \times \mathbf{B} = \frac{4\pi}{c} \mathbf{J} \ . \tag{8}$$

Eliminating the current yields a single equation for the equilibrium

$$\frac{1}{4\pi}\,\mathbf{B}\cdot\nabla\mathbf{B} = \nabla\left(p + \frac{B^2}{8\pi}\right) . \tag{9}$$

The orthogonality condition, Eq. (5), suggests that we take the projections along covariant bases:

$$(\mathbf{B}\cdot\nabla\mathbf{B})\cdot\frac{\partial\mathbf{x}}{\partial z^i} = B\frac{\partial B}{\partial z^i} + 4\pi\frac{\partial p}{\partial z^i} , \tag{10}$$

yielding three scalar conditions for equilibrium. First, we note that the lefthand side of Eq. (10) is expressed naturally in terms of Christoffel symbols of the first kind

$$(\mathbf{B}\cdot\nabla\mathbf{B})\cdot\frac{\partial\mathbf{x}}{\partial z^i} = \frac{1}{g}\big([33,i] + 2\iota[23,i] + \iota^2[22,i]\big) + \frac{g_{i3}+\iota g_{i2}}{\sqrt{g}}\partial_\ell\left(\frac{1}{\sqrt{g}}\right) \tag{11}$$

where

$$[ij,k] \doteq \frac{1}{2}\left(\frac{\partial g_{ik}}{\partial z^j} + \frac{\partial g_{jk}}{\partial z^i} - \frac{\partial g_{ij}}{\partial z^k}\right) \tag{12}$$

and $\partial_\ell = \partial/\partial z_3 + \iota\partial/\partial z_2$. From this result is it easy to show

$$\begin{aligned}\partial_\ell\left(\frac{g_{i3}+\iota g_{i2}}{\sqrt{g}}\right) - \frac{\partial}{\partial z^i}\left(\frac{g_{33}+2\iota g_{23}+\iota^2 g_{22}}{\sqrt{g}}\right)& \\ + \iota'\left(\frac{g_{23}+\iota g_{22}}{\sqrt{g}}\right)\delta_i^1 &= 4\pi\sqrt{g}p'\delta_i^1 ,\end{aligned} \tag{13}$$

where a prime denotes a derivative with respect to z^1.

2.3. Radial current

Setting $i = 2, 3$ gives the same result; namely, the condition for *zero radial current*:

$$\frac{\partial}{\partial z^2}\left(\frac{g_{33}+\iota g_{23}}{\sqrt{g}}\right) = \frac{\partial}{\partial z^3}\left(\frac{g_{23}+\iota g_{22}}{\sqrt{g}}\right) . \tag{14}$$

2.4. Force balance

Setting $i = 1$ gives the condition for *radial force balance*:

$$\begin{aligned}\partial_\ell\left(\frac{g_{13}+\iota g_{12}}{\sqrt{g}}\right) - \frac{\partial}{\partial z^1}\left(\frac{g_{33}+2\iota g_{23}+\iota^2 g_{22}}{\sqrt{g}}\right)& \\ + i'\left(\frac{g_{23}+\iota g_{22}}{\sqrt{g}}\right) &= 4\pi\sqrt{g}p' .\end{aligned} \tag{15}$$

Together, Eqns (14) and (15) are the scalar conditions for three-dimensional magnetostatic equilibrium.

2.5. Metric elements

Writing the position vector as

$$\mathbf{x} = R\sin\varphi\,\mathbf{e}_x + R\cos\varphi\,\mathbf{e}_y + Z\mathbf{e}_z \ , \tag{16}$$

the metric elements become

$$g_{33} = g_{\varphi\varphi} = \frac{\partial\mathbf{x}}{\partial\varphi}\cdot\frac{\partial\mathbf{x}}{\partial\varphi} = R^2 + \left(\frac{\partial R}{\partial\varphi}\right)^2 + \left(\frac{\partial Z}{\partial\varphi}\right)^2 \tag{17}$$

$$g_{22} = g_{\theta\theta} = \frac{\partial\mathbf{x}}{\partial\theta}\cdot\frac{\partial\mathbf{x}}{\partial\theta} = \left(\frac{\partial R}{\partial\theta}\right)^2 + \left(\frac{\partial Z}{\partial\theta}\right)^2 \tag{18}$$

$$g_{23} = g_{\theta\varphi} = \frac{\partial\mathbf{x}}{\partial\theta}\cdot\frac{\partial\mathbf{x}}{\partial\varphi} = \frac{\partial R}{\partial\theta}\frac{\partial R}{\partial\varphi} + \frac{\partial Z}{\partial\theta}\frac{\partial Z}{\partial\varphi} \tag{19}$$

$$g_{13} = g_{\chi\varphi} = \frac{\partial\mathbf{x}}{\partial\chi}\cdot\frac{\partial\mathbf{x}}{\partial\varphi} = \frac{\partial R}{\partial\chi}\frac{\partial R}{\partial\varphi} + \frac{\partial Z}{\partial\chi}\frac{\partial Z}{\partial\varphi} \tag{20}$$

$$g_{12} = g_{\chi\theta} = \frac{\partial\mathbf{x}}{\partial\chi}\cdot\frac{\partial\mathbf{x}}{\partial\theta} = \frac{\partial R}{\partial\chi}\frac{\partial R}{\partial\theta} + \frac{\partial Z}{\partial\chi}\frac{\partial Z}{\partial\theta} \ . \tag{21}$$

The Jacobian takes the form

$$\sqrt{g} = \frac{\partial\mathbf{x}}{\partial\chi}\cdot\frac{\partial\mathbf{x}}{\partial\theta}\times\frac{\partial\mathbf{x}}{\partial\varphi} = R\left(\frac{\partial R}{\partial\chi}\frac{\partial Z}{\partial\theta} - \frac{\partial R}{\partial\theta}\frac{\partial Z}{\partial\chi}\right) \ . \tag{22}$$

We can also associate poloidal and toroidal fields with the directions of the covariant bases; that is

$$\mathbf{B} = \mathbf{B}_p + \mathbf{B}_t \ , \tag{23}$$

where

$$\mathbf{B}_p = \frac{\iota}{\sqrt{g}}\frac{\partial\mathbf{x}}{\partial\theta} \ \longrightarrow B_p = \sqrt{\mathbf{B}_p\cdot\mathbf{B}_p} = \frac{\iota}{\sqrt{g}}\sqrt{g_{\theta\theta}} \ , \tag{24}$$

$$\mathbf{B}_t = \frac{1}{\sqrt{g}}\frac{\partial\mathbf{x}}{\partial\varphi} \ \longrightarrow B_t = \sqrt{\mathbf{B}_t\cdot\mathbf{B}_t} = \frac{1}{\sqrt{g}}\sqrt{g_{\varphi\varphi}} \ , \tag{25}$$

and

$$B = \frac{1}{\sqrt{g}}\sqrt{g_{\varphi\varphi} + \iota^2 g_{\theta\theta} + 2\iota g_{\theta\varphi}} \ . \tag{26}$$

3. The local equilibrium perspective

Solving the equilibrium equations globally is a formidable task [13] that is fraught with theoretical difficulties related to rational surfaces. Rational surfaces are singularities of the ideal system. In reality, the plasma pressure is a kinetic quantity through which dissipative effects appear. This dissipation provides the physical means to regularize the system, but to include dissipation rigorously (through the Fokker-Planck collision operator) would require solving an intractable kinetic system. The local equilibrium approach here offers a useful alternative to a global solution as we can focus, for example, on a single irrational q for which the flux surfaces should unambiguously exist.

3.1. Axisymmetric formulation

The Mercier-Luc [1] approach to axisymmetric local equilibrium requires the parametric specification of the flux surface via $R_s(\bar{\theta}_s)$ and $Z_s(\bar{\theta}_s)$, together with the poloidal field $B_{ps}(\bar{\theta}_s)$ on the surface. Here, $\bar{\theta}_s$ is a parametric angle that is not equal to the straight fieldline angle θ, and the subscript s refers to a reference surface. Miller's [4] innovation to this approach was to use a radially continuous form for R and Z valid not only on the surface, but also in the neighborhood of the surface. In this way B_{ps} (together with R_s and Z_s) can be computed from R, Z and their derivatives. However, once B_{ps} is specified, the global forms for R, Z must be discarded and all nonlocal behavior subsequently determined by solution of the current and force balance equations. This approach allows one to not only to specify the shape, but also effects that depend on the derivative of the shape (Shafranov shift, elongation shear, etc).

3.2. Nonaxisymmetric formulation

To generalize Miller's approach to nonaxisymmetric systems, we first specify a parameterization of the flux surface $R_p(\bar{\theta},\bar{\varphi},\bar{r})$ and $Z_p(\bar{\theta},\bar{\varphi},\bar{r})$, where the subscript p means *parameterized*. These forms are taken to hold both on the reference surface as well as in the neighborhood of that surface. The explicit form of the parameterization is not important. Some models for the 2D case are discussed in Ref. [5]. This parameterization is then used to compute three surface functions R_s, Z_s and J_s, where

$$R_s(\bar{\theta}_s,\bar{\varphi}_s) = R_p(\bar{\theta}_s,\bar{\varphi}_s,\bar{r}_s) \tag{27}$$

$$Z_s(\bar{\theta}_s,\bar{\varphi}_s) = Z_p(\bar{\theta}_s,\bar{\varphi}_s,\bar{r}_s) \tag{28}$$

$$J_s(\bar{\theta}_s,\bar{\varphi}_s) = \; R_p \left(\frac{\partial R_p}{\partial \bar{r}} \frac{\partial Z_p}{\partial \bar{\theta}} - \frac{\partial R_p}{\partial \bar{\theta}} \frac{\partial Z_p}{\partial \bar{r}} \right) \Bigg|_{\mathbf{x}=\mathbf{x}_s} . \tag{29}$$

In terms of the surface functions, we can write the Jacobian on the surface as

$$\sqrt{g_s} = \frac{J_s(\bar{\theta}_s,\bar{\varphi}_s)}{d\chi/dr} \; \frac{\partial \bar{\theta}}{\partial \theta} \Bigg|_{\mathbf{x}=\mathbf{x}_s} . \tag{30}$$

Note that this approach ensures that the surface Jacobian is consistent with radial dependence of the parameterization. This is in contrast to Hegna's treatment [6], for which the Jacobian is not determined by the surface parameterization. This feature is also discussed by Boozer [12]. Now, knowing the three surface functions, we *discard* the parameterization (R_p, Z_p). In Eq. (30), $d\chi/dr \doteq r B_{\rm unit}$, where $B_{\rm unit}$ is the effective magnetic field strength on the flux surface [14] and r is a suitably chosen length. In 2D, r is the half-width of the flux-surface at the elevation of the centroid (just a very general definition of the minor radius). In 3D, r can be defined as the toroidal average of the 2D definition, but different definitions are possible. In general, small alterations in the definition of r will give rise to small alterations in $B_{\rm unit}$. In the absence of a global equilibrium, $B_{\rm unit}$ is a free parameter as explained in Ref. [15]. The

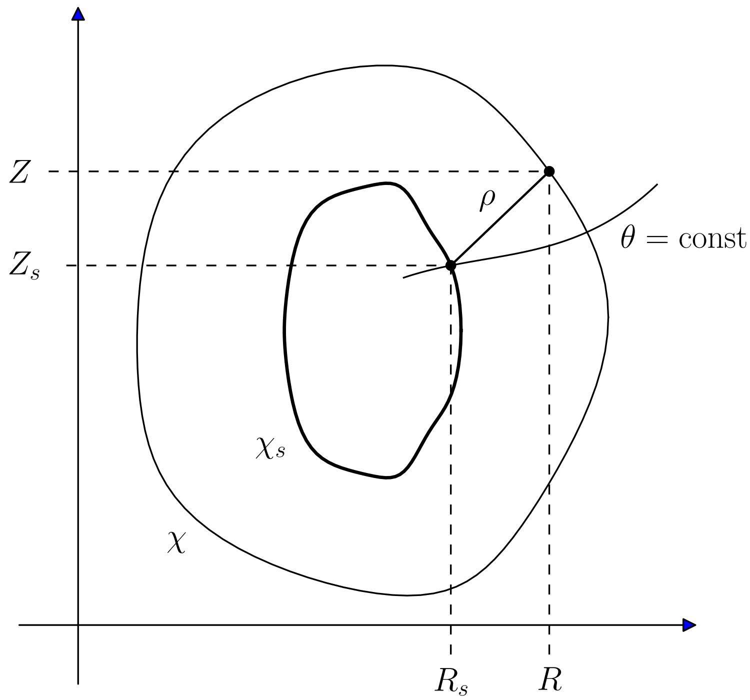

Figure 1: Illustration of coordinate system defined in Eqns (34) and (35) for a fixed toroidal angle φ_s. Whereas the reference flux surface, χ_s, has $\rho = 0$ everywhere on the surface, an adjacent flux surface, χ, is not a surface of constant ρ. Further, the segment labeled ρ, on which $\theta_s = \text{const}$, is not the same as the arc $\theta = \text{const}$.

parametric coordinates $(\bar{\theta}, \bar{\varphi}, \bar{r})$ are related to the straight fieldline coordinates via the transformation

$$\bar{r} = r \; , \tag{31}$$

$$\bar{\theta} = \bar{\theta}(r, \theta, \varphi) \; , \tag{32}$$

$$\bar{\varphi} = \varphi \; . \tag{33}$$

We emphasize that the explicit form of the transformation is not yet known. Later, it will be determined by the condition of zero radial current. The strategy to obtain a local equilibrium solution will be to first represent R and Z both on the reference surface, and in the neighborhood of that surface, in $(\rho, \theta_s, \varphi_s)$ coordinates via

$$R(r, \theta, \varphi) = R_s(\theta_s, \varphi_s) + \rho \cos u(\theta_s, \varphi_s) \; , \tag{34}$$

$$Z(r, \theta, \varphi) = Z_s(\theta_s, \varphi_s) + \rho \sin u(\theta_s, \varphi_s) \; . \tag{35}$$

The relation between r (or equivalently, χ) and ρ is not known *a priori* and must be computed. An illustration of the coordinate system is shown in Fig. 1. In the equations above, u is the frame angle of the curve represented by the intersection of the reference flux surface and the toroidal plane $\varphi = \varphi_s$. Specifically,

$$\sin u = -\frac{1}{\ell_\theta}\frac{\partial R_s}{\partial \theta_s} \quad \text{and} \quad \cos u = \frac{1}{\ell_\theta}\frac{\partial Z_s}{\partial \theta_s} \ , \tag{36}$$

where

$$\ell_\theta^2 = \left(\frac{\partial R_s}{\partial \theta_s}\right)^2 + \left(\frac{\partial Z_s}{\partial \theta_s}\right)^2 \ . \tag{37}$$

We write the connection between the original (χ, θ, φ)-coordinates and the non-flux $(\rho, \theta_s, \varphi_s)$-coordinates via an expansion in the small parameter ρ

$$\chi = \chi_s + \rho\,\chi_1(\theta_s, \varphi_s) + \rho^2\,\chi_2(\theta_s, \varphi_s) + \cdots \ , \tag{38}$$

$$\theta = \theta_s + \rho\,\theta_1(\theta_s, \varphi_s) + \cdots \ , \tag{39}$$

$$\varphi = \varphi_s \ . \tag{40}$$

Derivatives can then be expressed in terms of the free functions χ_1, χ_2 and θ_1 according to

$$\frac{\partial}{\partial \chi} \sim \frac{1}{\chi_1}\left[1 + \rho\left(\frac{\partial \ln \chi_1}{\partial \theta_s} - \delta\chi\right)\right]\frac{\partial}{\partial \rho} - \delta\theta\left[1 - \rho\left(\delta\chi + \chi_1\frac{\partial\,\delta\theta}{\partial \theta_s}\right)\right]\frac{\partial}{\partial \theta_s} \ , \tag{41}$$

$$\frac{\partial}{\partial \theta} \sim -\left(\rho\,\frac{\partial \ln \chi_1}{\partial \theta_s}\right)\frac{\partial}{\partial \rho} + \left(1 - \rho\chi_1\frac{\partial\,\delta\theta}{\partial \theta_s}\right)\frac{\partial}{\partial \theta_s} \ , \tag{42}$$

$$\frac{\partial}{\partial \varphi} \sim -\left(\rho\,\frac{\partial \ln \chi_1}{\partial \varphi_s}\right)\frac{\partial}{\partial \rho} - \left(\rho\,\chi_1\frac{\partial\,\delta\theta}{\partial \varphi_s}\right)\frac{\partial}{\partial \theta_s} + \frac{\partial}{\partial \varphi_s} \ . \tag{43}$$

where

$$\delta\theta \doteq \frac{\theta_1}{\chi_1} \quad \text{and} \quad \delta\chi \doteq \frac{2\chi_2}{\chi_1^2} \ . \tag{44}$$

Whereas determination of χ_1 is straightforward, we must solve a system of differential equations for $\delta\theta$ and $\delta\chi$. To illustrate the expansion procedure, we write

$$\sqrt{g} \sim \frac{\ell_\theta R_s}{\chi_1}\left[1 + \rho\left(\frac{1}{r_c} + \frac{\cos u}{R_s} - \delta\chi - \chi_1\frac{\partial\,\delta\theta}{\partial \theta_s}\right)\right] + \mathcal{O}(\rho^2) \ . \tag{45}$$

This implies that

$$\chi_1 = \frac{\ell_\theta R_s}{\sqrt{g_s}} \tag{46}$$

where $\sqrt{g_s}$ is given by Eq. (30).

4. Zeroth-order equilibrium

4.1. Nonlinear equation for the mapping

In zeroth order, the condition for zero radial current becomes

$$\mathcal{C} = \frac{\partial}{\partial \theta}\left(\frac{N_0}{\sqrt{g_s}}\right) - \frac{\partial}{\partial \varphi}\left(\frac{M_0}{\sqrt{g_s}}\right) = 0 \tag{47}$$

where

$$M_0 = \iota_s \ell_\theta^2 + g_{\theta\varphi,s} \ , \tag{48}$$

$$N_0 = R_s^2 + \ell_\varphi^2 + \iota_s g_{\theta\varphi,s} \ , \tag{49}$$

$$\ell_\varphi^2 = \left(\frac{\partial R_s}{\partial \varphi_s}\right)^2 + \left(\frac{\partial Z_s}{\partial \varphi_s}\right)^2 \ . \tag{50}$$

In these expressions, $g_{\theta\varphi,s}$ is the metric element defined in Sec. 2.5 evaluated on the reference surface. The subtlety associated with Eq. (47) is that R_s, Z_s and J_s are explicit functions of an unknown mapping function $\bar{\theta}$. For this reason, it is necessary to evaluate the derivatives in the fieldline following coordinates using the chain rule

$$\frac{\partial}{\partial \theta_s} = \frac{\partial \bar{\theta}}{\partial \theta_s} \frac{\partial}{\partial \bar{\theta}} \tag{51}$$

$$\frac{\partial}{\partial \varphi_s} = \frac{\partial \bar{\theta}}{\partial \varphi_s} \frac{\partial}{\partial \bar{\theta}} + \frac{\partial}{\partial \bar{\varphi}} \ . \tag{52}$$

Thus, Eq. (47) is a nonlinear partial differential equation for the coordinate transformation $\bar{\theta} = \bar{\theta}(\theta_s, \varphi_s)$.

4.2. Numerical method for calculation of $\bar{\theta}(\theta, \varphi)$

Equation (47) is a nonstandard type of equation that is challenging to solve numerically. In what follows we outline a numerical method for solution. The foundation of the method is the expansion

$$\bar{\theta} = \theta + \sum_{m=0}^{N_\theta} \sum_{n=0}^{N_\varphi} \Big\{ \sin(m\theta) \left[a_{mn} \cos(n\varphi) + b_{mn} \sin(n\varphi) \right] + \cos(m\theta) \left[c_{mn} \cos(n\varphi) + d_{mn} \sin(n\varphi) \right] \Big\} \tag{53}$$

The conditions on the Fourier coefficients are

$$a_{mn} = 0 \qquad \text{if } m = 0 \ , \tag{54}$$

$$b_{mn} = 0 \qquad \text{if } m = 0 \text{ or } n = 0 \ , \tag{55}$$

$$c_{mn} = 0 \qquad \text{if } m + n = 0 \ , \tag{56}$$

$$d_{mn} = 0 \qquad \text{if } n = 0 \ . \tag{57}$$

The condition on c_{00} is arbitrary and sets an overall constant to zero. We can write this rather cumbersome expression more compactly as

$$\bar{\theta} = \theta + \sum_{p=0}^{N-1} \alpha_p \mathcal{F}_p(\theta, \varphi) \tag{58}$$

where p is the lumped Fourier index, $N = 1 + 4N_\theta N_\varphi + 2(N_\theta + N_\varphi)$, and $\mathcal{F}_p$ is defined in Table 1. By taking the residual to be orthogonal to the finite Fourier

Table 1: Explicit description of 2D Fourier basis, where $\omega_{mn} \doteq 2(N_\theta + N_\varphi) + 4(n-1) + 4N_\varphi(m-1)$. Note that all entries assume $1 \le m \le N_\theta$ and $1 \le n \le N_\varphi$.

Coefficient	p	$\mathcal{F}_p(\theta,\varphi)$
c_{00}	0	1
a_{m0}	m	$\sin(m\theta)$
c_{m0}	$N_\theta + m$	$\cos(m\theta)$
c_{0n}	$2N_\theta + n$	$\cos(n\varphi)$
d_{0n}	$2N_\theta + N_\varphi + n$	$\sin(n\varphi)$
a_{mn}	$1 + \omega_{mn}$	$\sin(m\theta)\cos(n\varphi)$
b_{mn}	$2 + \omega_{mn}$	$\sin(m\theta)\sin(n\varphi)$
c_{mn}	$3 + \omega_{mn}$	$\cos(m\theta)\cos(n\varphi)$
d_{mn}	$4 + \omega_{mn}$	$\cos(m\theta)\sin(n\varphi)$

series, and using integration by parts to ensure all derivatives are carried out analytically, we can write the equations for the undetermined coefficients α_p as

$$\int_0^{2\pi} d\theta \int_0^{2\pi} d\varphi \left[\frac{\partial \mathcal{F}_p}{\partial \varphi} \left(\frac{M_0}{\sqrt{g_s}} \right) - \frac{\partial \mathcal{F}_p}{\partial \theta} \left(\frac{N_0}{\sqrt{g_s}} \right) \right] = 0 \ . \tag{59}$$

Note that $p = 0$ is trivially satisfied, indicating that $c_{00} = \alpha_0$ is arbitrary. To evaluate the integrals we use numerical integration. Because the range of integration is over a periodic interval, equally-spaced nodes are optimal and give spectral accuracy. Specifically, we use the rule

$$\int_0^{2\pi} d\theta \int_0^{2\pi} d\varphi \, f(\theta,\varphi) \to \frac{1}{M_\theta M_\varphi} \sum_{i=0}^{M_\theta - 1} \sum_{j=0}^{M_\varphi - 1} f(\theta_i, \varphi_j) \tag{60}$$

where $\theta_i = 2\pi i / M_\theta$, $\varphi_j = 2\pi j / M_\varphi$, $M_\theta = 2(N_\theta + 1)$ and $M_\varphi = 2(N_\varphi + 1)$. The result is a spectrally-accurate system of $N - 1$ nonlinear algebraic equations for the coefficients $(\alpha_1, \ldots, \alpha_N)$. To solve the nonlinear system, we use the HYBRD1 routine from MINPACK [16].

4.3. Example: an axisymmetric shifted circle

It is useful to develop some intuition, and to contrast the differences between the present work and Ref. [6], by examining the zero radial current condition for the simple case of an axisymmetric circular plasma. We begin with a nonlocal parameterization $\{R_p, Z_p\}$ (see Section 3.2) for a shifted circle

$$R_p(r,\bar\theta) = R_0(r) + r\cos\bar\theta \ , \tag{61}$$

$$Z_p(r,\bar\theta) = r\sin\bar\theta \ . \tag{62}$$

The implies the surface parameterization $\{R_s, Z_s, J_s\}$, where

$$R_s(\bar\theta_s) = R_{0s} + r_s \cos\bar\theta_s \ , \tag{63}$$

$$Z_s(\bar\theta_s) = r_s \sin\bar\theta_s \ , \tag{64}$$

$$J_s(\bar\theta_s) = r_s R_s \left(1 + R_0' \cos\bar\theta_s\right) \ . \tag{65}$$

Note the explicit appearance of the Shafranov shift, R_0', in J_s. In the axisymmetric case, Eq. (47) is solved via a trivial integration

$$\frac{\partial}{\partial\theta_s}\left(\frac{R_s^2}{\sqrt{g_s}}\right) = 0 \quad \rightarrow \quad \frac{R_s^2}{\sqrt{g_s}} = I_s \ , \tag{66}$$

where I_s is a constant of integration. Inserting J_s into the expression above yields a nonlinear, first-order ODE for the parametric angle $\bar\theta_s(\theta_s)$:

$$\frac{R_{0s}}{r_s} + \cos\bar\theta_s = \frac{I_s}{d\chi/dr}\left(1 + R_0'\cos\bar\theta_s\right)\frac{\partial\bar\theta_s}{\partial\theta_s} \ . \tag{67}$$

This equation can be solved for arbitrary R_0'. However, without the freedom to specify the parametric angle, there is no mechanism to explicitly set the Shafranov shift (or more generally, the gradient of the shape). For example, in the absence of a parametric angle, the surface parameterization would be

$$R_s(\theta_s) = R_{0s} + r_s \cos\theta_s \ , \tag{68}$$

$$Z_s(\theta_s) = r_s \sin\theta_s \ . \tag{69}$$

Attempting to use the previous Jacobian, J_s, would yield a current constraint,

$$\frac{R_{0s}}{r_s} + \cos\theta_s = \frac{I_s}{d\chi/dr}\left(1 + R_0'\cos\theta_s\right) \ , \tag{70}$$

for which a solution is possible only if $R_0' = r_s/R_{0s}$. Thus, without the use of a parametric angle, there does not appear to be a systematic way to control the gradient of the flux-surface shape. This provides the clearest contrast between the present work and the treatment in Ref. [6]. In the latter case, the gradient of the shape is not defined in the parameterization, and Eq. (47) is viewed as a linear equation for $\sqrt{g_s}$. Conversely, in the present case, the gradient of the shape is defined by the parameterization, and this extra freedom makes Eq. (47) a nonlinear PDE for $\bar\theta_s$.

By considering the limit $\epsilon = r_s/R_{0s} \to 0$, and ordering $R_0' \sim \mathcal{O}(\epsilon)$, we can solve Eq. (67) to obtain

$$\frac{I_s}{d\chi/dr} \sim \frac{1}{\epsilon} + \frac{1}{2}\left(\epsilon + R_0' - \frac{{R_0'}^2}{\epsilon}\right) + \mathcal{O}(\epsilon^3) \ , \tag{71}$$

$$\bar\theta_s \sim \theta_s + (\epsilon - R_0')\sin\theta_s + \frac{1}{4}\left(\epsilon^2 - \epsilon R_0' - {R_0'}^2 +\right)\sin 2\theta_s + \mathcal{O}(\epsilon^3) \ . \tag{72}$$

This formula can be used as a simple check on the accuracy of the numerical solution of Eq. (53), or to provide an initial guess for the rootfinder.

5. First-order equilibrium

5.1. Linear equations for current and force balance

After lengthy algebra, we find coupled linear differential equations for the functions $\delta\theta$ and $\delta\chi$

$$\begin{bmatrix} A_{11} & A_{12} \\ A_{21} & A_{22} \end{bmatrix} \begin{bmatrix} \delta\theta \\ \delta\chi \end{bmatrix} = \begin{bmatrix} S_1 \\ S_2 \end{bmatrix} \tag{73}$$

where

$$A_{11} f = \frac{M_0}{\sqrt{g_s}} \frac{\partial f}{\partial \varphi_s} - \frac{N_0}{\sqrt{g_s}} \frac{\partial f}{\partial \theta_s} \tag{74}$$

$$A_{12} f = -\frac{N_0 + \iota_s M_0}{\sqrt{g_s}} f \tag{75}$$

$$A_{21} f = \frac{\partial}{\partial \theta_s} \left(\frac{-2M_0 + \iota_s \ell_\theta^2}{\sqrt{g_s}} \frac{\partial f}{\partial \ell_s} + \frac{N_0 + \iota_s M_0}{\sqrt{g_s}} \frac{\partial f}{\partial \theta_s} \right) + \frac{\partial}{\partial \varphi_s} \left(\frac{\ell_\theta^2}{\sqrt{g_s}} \frac{\partial f}{\partial \ell_s} \right) - \left[\frac{M_0}{\sqrt{g_s}}, f \right] \tag{76}$$

$$A_{22} f = \frac{\partial}{\partial \theta_s} \left(\frac{N_0}{\sqrt{g_s}} f \right) - \frac{\partial}{\partial \varphi_s} \left(\frac{M_0}{\sqrt{g_s}} f \right) \tag{77}$$

$$S_1 = 4\pi p' \sqrt{g_s} + \frac{\delta N_0 + \iota_s \delta M_0}{\chi_1 \sqrt{g_s}} - \frac{\partial}{\partial \ell_s} \left(\frac{[R_s, Z_s]}{\ell_\theta \chi_1 \sqrt{g_s}} \right) \tag{78}$$

$$S_2 = \frac{\partial}{\partial \varphi_s} \left(\frac{\delta M_0}{\chi_1 \sqrt{g_s}} \right) - \frac{\partial}{\partial \theta_s} \left(\frac{\delta N_0}{\chi_1 \sqrt{g_s}} \right) . \tag{79}$$

In these equations we have defined the Poisson bracket

$$[f, g] \doteq \frac{\partial f}{\partial \theta_s} \frac{\partial g}{\partial \varphi_s} - \frac{\partial f}{\partial \varphi_s} \frac{\partial g}{\partial \theta_s} , \tag{80}$$

and the functions

$$\delta M_0 = \frac{\ell_\theta^2}{r_\varphi} + P_\theta + \iota_s \frac{2\ell_\theta^2}{r_\theta} + \chi_1 \iota_s \ell_\theta^2 - M_0 \eta \tag{81}$$

$$\delta N_0 = 2R_s \cos u + \iota_s \frac{\ell_\theta^2}{r_\varphi} + 2P_\varphi + P_\theta + \chi_1 \iota' g_{\theta\varphi,s} - N_0 \eta \tag{82}$$

$$\eta = \frac{1}{r_\theta} + \frac{\cos u}{R_s} . \tag{83}$$

5.2. Numerical method for solution

We can solve the linear system of differential equations, Eq. (73), numerically by converting it to a matrix system for the spectral expansion coefficients. That is,

$$\delta\theta = \sum_{p=0}^{N-1} \delta\theta_p \mathcal{F}_p \tag{84}$$

$$\delta\chi = \sum_{p=0}^{N-1} \delta\chi_p \mathcal{F}_p \tag{85}$$

with the corresponding block matrix system

$$\begin{bmatrix} A_{11}^{pp'} & A_{12}^{pp'} \\ A_{21}^{pp'} & A_{22}^{pp'} \end{bmatrix} \begin{bmatrix} \delta\theta_{p'} \\ \delta\chi_{p'} \end{bmatrix} = \begin{bmatrix} S_1^p \\ S_2^p \end{bmatrix} . \tag{86}$$

The blocks are

$$A_{11}^{pp'} = \int_0^{2\pi} d\theta \int_0^{2\pi} d\varphi \, \mathcal{F}_p \left(\frac{M_0}{\sqrt{g_s}} \frac{\partial \mathcal{F}_{p'}}{\partial\varphi} - \frac{N_0}{\sqrt{g_s}} \frac{\partial \mathcal{F}_{p'}}{\partial\theta} \right) \tag{87}$$

$$A_{12}^{pp'} = -\int_0^{2\pi} d\theta \int_0^{2\pi} d\varphi \left(\frac{N_0 + \iota_s M_0}{\sqrt{g_s}} \right) \mathcal{F}_p \mathcal{F}_{p'} \tag{88}$$

$$A_{21}^{pp'} = \int_0^{2\pi} d\theta \int_0^{2\pi} d\varphi \left\{ \left(\frac{2M_0 - \iota_s \ell_\theta^2}{\sqrt{g_s}} \right) \frac{\partial \mathcal{F}_p}{\partial\theta_s} \frac{\partial \mathcal{F}_{p'}}{\partial\ell_s} - \left(\frac{N_0 + \iota_s M_0}{\sqrt{g_s}} \right) \frac{\partial \mathcal{F}_p}{\partial\theta_s} \frac{\partial \mathcal{F}_{p'}}{\partial\theta_s} \right. \tag{89}$$

$$\left. - \frac{\ell_\theta^2}{\sqrt{g_s}} \frac{\partial \mathcal{F}_p}{\partial\varphi_s} \frac{\partial \mathcal{F}_{p'}}{\partial\ell_s} - \frac{M_0}{\sqrt{g_s}} \left[\mathcal{F}_p, \mathcal{F}_{p'} \right] \right\} \tag{90}$$

$$A_{22}^{pp'} = A_{11}^{p'p} \tag{91}$$

$$S_1^p = \int_0^{2\pi} d\theta \int_0^{2\pi} d\varphi \left\{ \left(4\pi p' \sqrt{g_s} + \frac{\delta N_0 + \iota_s \delta M_0}{\chi_1 \sqrt{g_s}} \right) \mathcal{F}_p - \frac{\partial \mathcal{F}_p}{\partial\ell_s} \left(\frac{[R_s, Z_s]}{\ell_\theta \chi_1 \sqrt{g_s}} \right) \right\} \tag{92}$$

$$S_2^p = \int_0^{2\pi} d\theta \int_0^{2\pi} d\varphi \left[\frac{\partial \mathcal{F}_p}{\partial\theta_s} \left(\frac{\delta N_0}{\chi_1 \sqrt{g_s}} \right) - \frac{\partial \mathcal{F}_p}{\partial\varphi_s} \left(\frac{\delta M_0}{\chi_1 \sqrt{g_s}} \right) \right] . \tag{93}$$

The discrete form of the helical derivative $\partial_\ell = \partial_\varphi + \iota_s \partial_\theta$ will vanish if the condition $n \pm \iota m = 0$, or equivalently $nq_s \pm m = 0$. If this occurs for some pair (m, n), then the block matrix in Eq. (86) will be singular. Because the local equilibrium method treats only a single surface at a time, one can simply avoid regions for which q is close to a low-order rational. This ensures the matrix problem is nonsingular. Alternatively, in the case of high-order rational surfaces (for example $q = 21/20$) one can limit the spectral element basis so that the singularity is associated with higher harmonics than those retained in the numerical solution.

5.3. Numerical check in the axisymmetric limit

To verify the calculation of radial force balance, we can compare the solution of equation (73) with the standard Miller formulation [5]. We note that the

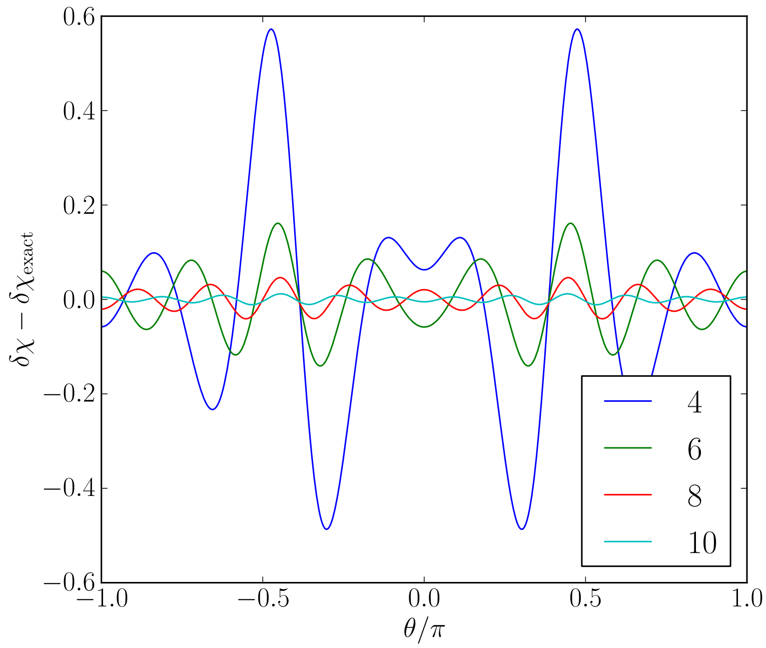

Figure 2: Accuracy check of the present spectral solver against an independent implementation of the Miller 2D equilibrium solver. The Miller solver with 1001 gridpoints in θ was used to generate $\delta\chi_{\rm exact}$. The plot shows rapid convergence as of the spectral solver for $N_\theta = 4, 6, 8, 10$.

poloidal flux expansion coefficients ψ_1 and ψ_2 given by Eqns (64) and (65) in Ref. [5] are related to χ_1 and χ_2 by the following relations:

$$\chi_1 = \psi_1/\iota_s \quad \text{and} \quad \delta\chi = 2\,\frac{\chi_2}{\chi_1^2} = 2\iota_s\frac{\psi_2}{\psi_1^2} + \frac{s}{r^2} \tag{94}$$

where $s = (r/q)dq/dr$ is the magnetic shear. In Fig. 2 we compare the spectral solution, Eq. (86), with the finite-difference solver reported in Ref. [5]. This plot verifies the correctness as well as the convergence of the present method in the axisymmetric limit.

6. Expressions for Differential Operators

The following are useful quantities for kinetic calculations in terms of the metric components.

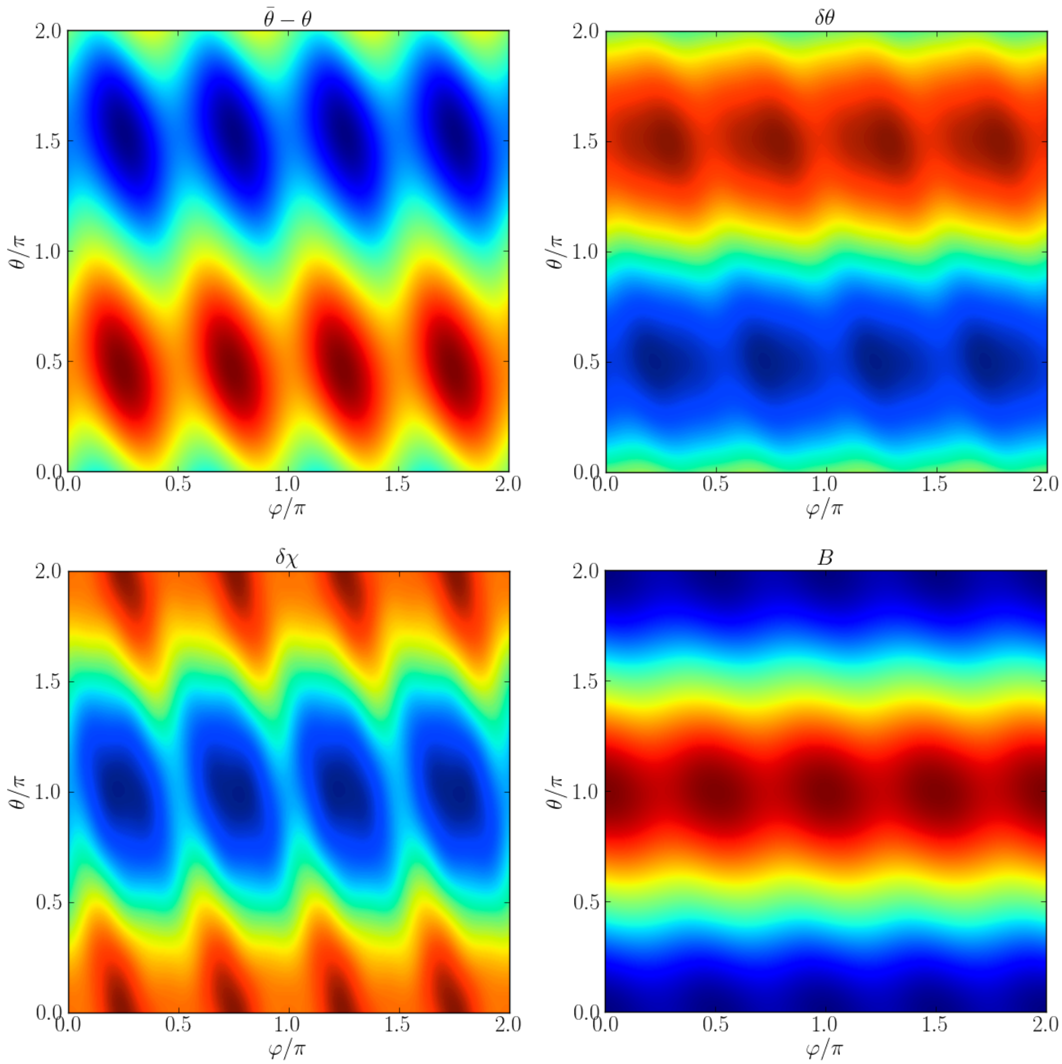

Figure 3: Contour maps of $\bar{\theta}-\theta$, $\delta\theta$, $\delta\chi$, and the resulting magnetic field B on the surface for flux-surface shape $R_p = R_0(r) + r\cos\bar{\theta} + \delta(r)\cos(2\bar{\theta} - 4\bar{\varphi})$, $Z_p = r\sin\bar{\theta} + \delta(r)\sin(2\bar{\theta} - 4\bar{\varphi})$ on the surface $r = r_s = 0.5\,a$. Here, $R_0(r) = 3\,a$, $\delta(r) = 0.015\,a$, $q_s = 2.11$ and $s = 1$.

$$\mathbf{B}\cdot\nabla\theta\bigg|_s = \frac{\iota_s}{\sqrt{g_s}} \tag{95}$$

$$\mathbf{B}\cdot\nabla\varphi\bigg|_s = \frac{1}{\sqrt{g_s}} \tag{96}$$

$$\mathbf{B}\times\nabla B\cdot\nabla\chi\bigg|_s = \frac{1}{g_s}\left[-\frac{\partial B_s}{\partial\theta_s}\left(g_{\varphi\varphi,s}+\iota_s g_{\theta\varphi,s}\right)+\frac{\partial B_s}{\partial\varphi_s}\left(g_{\theta\varphi,s}+\iota_s g_{\theta\theta,s}\right)\right] \tag{97}$$

$$\mathbf{B}\times\nabla B\cdot\nabla\theta\bigg|_s = \frac{1}{g_s}\left[\left(\frac{B_1}{\chi_1}-\delta\theta\frac{\partial B_s}{\partial\theta_s}\right)\left(g_{\varphi\varphi,s}+\iota_s g_{\theta\varphi,s}\right)-\frac{\partial B_s}{\partial\varphi_s}\left(g_{\chi\varphi,s}+\iota_s g_{\chi\theta,s}\right)\right] \tag{98}$$

$$\mathbf{B}\times\nabla B\cdot\nabla\varphi\bigg|_s = \frac{1}{g_s}\left[-\left(\frac{B_1}{\chi_1}-\delta\theta\frac{\partial B_s}{\partial\theta_s}\right)\left(g_{\theta\varphi,s}+\iota_s g_{\theta\theta,s}\right)+\frac{\partial B_s}{\partial\theta_s}\left(g_{\chi\varphi,s}+\iota_s g_{\chi\theta,s}\right)\right] \tag{99}$$

where B_1 is defined by the ρ expansion of B; namely,

$$B \sim B_s + \rho B_1(\theta_s,\varphi_s) + \mathcal{O}(\rho^2)\ . \tag{100}$$

An example numerical solution of Eqns (59) and (86) for a 3D local equilibrium is shown in Fig. 3, along with a contour plot of the resulting magnetic field strength B_s.

7. Summary

In the preceding sections, we have developed all the machinery necessary to evaluate first-order differential operators in the neighborhood of a reference three-dimensional flux surface using a local equilibrium method. This method is a generalization of the very popular Miller approach in two dimensions. Below we summarize the basic steps required to complete this procedure:

1. Choose forms for (R_p, Z_p) valid on (and in the neighborhood of) a reference flux surface.
2. Evaluate (R_s, Z_s, J_s) on the reference surface as described in Sec. 3.2, then discard the parameterization (R_p, Z_p).
3. Solve Eq. (59) for the coefficients $(\alpha_1, \ldots, \alpha_N)$ to obtain $\bar{\theta}(\theta_s)$.
4. Solve Eq. (86) for the coefficients $(\delta\theta_p, \delta\chi_p)$.
5. Use the quantities computed in the previous steps to evaluate, for example, the differential operators described in Sec. 6.

Appendix A. Transformation to Boozer coordinates

The magnetic field, when written in Boozer coordinates $(\chi, \theta_B, \varphi_B)$, takes the form

$$\mathbf{B} = B_\theta(\chi)\nabla\theta_B + B_\varphi(\chi)\nabla\varphi_B + B_\chi(\chi,\theta_B,\varphi_B)\nabla\chi\ . \tag{A.1}$$

Dotting the above (contravariant) form of $\mathbf{B}$ with the covariant form gives the familiar result $B^2 = (\iota I + J)/\sqrt{g_B}$, where $\sqrt{g_B}$ is the Boozer Jacobian. Since the Boozer angles are themselves straight fieldline angles, they can be related to the straight fieldline angles of the present work according to

$$\theta = \theta_B + \iota\omega(\chi, \theta_B, \varphi_B) \ , \tag{A.2}$$

$$\varphi = \varphi_B + \omega(\chi, \theta_B, \varphi_B) \ , \tag{A.3}$$

where ω is a doubly-periodic generating function. Relating Eqns (A.1) and (1), we find that the equations determining ω are

$$\mathbf{B} \cdot \frac{\partial \mathbf{x}}{\partial \theta} = \frac{1}{\sqrt{g}} (g_{\theta\varphi} + \iota g_{\theta\theta}) = B_\theta - \frac{\partial \omega}{\partial \theta} (B_\varphi + \iota B_\theta) \ , \tag{A.4}$$

$$\mathbf{B} \cdot \frac{\partial \mathbf{x}}{\partial \varphi} = \frac{1}{\sqrt{g}} (g_{\varphi\varphi} + \iota g_{\theta\varphi}) = B_\varphi - \frac{\partial \omega}{\partial \varphi} (B_\varphi + \iota B_\theta) \ , \tag{A.5}$$

$$\mathbf{B} \cdot \frac{\partial \mathbf{x}}{\partial \chi} = \frac{1}{\sqrt{g}} (g_{\chi\varphi} + \iota g_{\chi\theta}) = B_\chi - \frac{\partial \omega}{\partial \chi} (B_\varphi + \iota B_\theta) \ . \tag{A.6}$$

The first two equations show that the condition for zero radial current, Eq. (14), is satified by arbitrary B_θ and B_φ. From these relations, we see at once that the flux functions in Eq. (A.3) can be expressed as the integrals

$$B_\theta(\chi) = \frac{1}{2\pi} \int_0^{2\pi} d\theta \, \frac{g_{\theta\varphi} + \iota g_{\theta\theta}}{\sqrt{g}} \ , \tag{A.7}$$

$$B_\varphi(\chi) = \frac{1}{2\pi} \int_0^{2\pi} d\varphi \, \frac{g_{\varphi\varphi} + \iota g_{\theta\varphi}}{\sqrt{g}} \ . \tag{A.8}$$

Once these flux-functions are determined, the value of ω on the surface can then be computed via the solution of the first two differential equations. To obtain B_χ and the variation of ω off the surface, the formalism of Sec. 3.2 must be used. Finally, we remark that in the case of an unshifted axisymmetric circle, we find

$$B_{\theta s} = \iota_s r_s^2 B_{\text{unit}} \left\langle \frac{1}{R_s} \right\rangle \ , \tag{A.9}$$

$$B_{\varphi s} = B_{\text{unit}} \left\langle \frac{1}{R_s} \right\rangle^{-1} \ , \tag{A.10}$$

$$\theta_{Bs} = \theta_s \ , \tag{A.11}$$

$$\varphi_{Bs} = \varphi_s \ , \tag{A.12}$$

$$\omega_s = 0 \ , \tag{A.13}$$

where the angle brackets denote an average over θ.

Acknowledgements

This material is based upon work supported by the U.S. Department of Energy, Office of Science, Office of Fusion Energy Sciences, Theory program, under Award DE-FG02-95ER54309 and by the Edge Simulation Laboratory project under Grant DE-FC02-06ER54873.

References

[1] C. Mercier, N. Luc, Tech. rep., Commission of the European Communities, Report No. EUR-5127e 140, Brussels (1974).

[2] J. Greene, M. Chance, Nucl. Fusion 21 (1981) 453.

[3] C. Bishop, P. Kirby, J. Connor, R. Hastie, J. Taylor, Ideal MHD ballooning stability in the vicinity of a separatrix, NF 24 (1984) 1579.

[4] R. Miller, M. Chu, J. Greene, Y. Lin-liu, R. Waltz, Noncircular, finite aspect ratio, local equilibrium model, Phys. Plasmas 5 (1998) 973.

[5] J. Candy, C. Holland, R. Waltz, M. Fahey, E. Belli, Tokamak profile prediction using direct gyrokinetic and neoclassical simulation, Phys. Plasmas 16 (2009) 060704.

[6] C. Hegna, Local three-dimensional magnetostatic equilibria, Phys. Plasmas 7 (2000) 3921.

[7] S. Hirshman, K. Shaing, W. van Rij, J. C.O. Beasley, J. E.C. Crume, Plasma transport coefficients for nonsymmetric toroidal confinement systems, Phys. Fluids 29 (1986) 2951.

[8] W. van Rij, S. Hirshman, Variational bounds for transport coefficients in three-dimensional toroidal plasmas, Phys. Fluids B 1 (1989) 563.

[9] P. Xanthopoulos, F. Merz, T. Görler, F. Jenko, Nonlinear Gyrokinetic Simulations of Ion-Temperature-Gradient Turbulence for the Optimized Wendelstein 7-X Stellarator, Phys. Rev. Lett. 99 (2007) 035002.

[10] J. Baumgaertel, E. Belli, W. Dorland, W. Guttenfelder, G. Hammett, D. Mikkelsen, G. Rewoldt, W. Tang, P. Xanthopoulos, Simulating gyrokinetic microinstabilities in stellarator geometry with GS2, Phys. Plasmas 18 (2011) 122301.

[11] T. Bird, C. Hegna, A model for microinstability destabilization and enhanced transport in the presence of shielded 3d mangetic perturbations, Nucl. Fusion 53 (2013) 013004.

[12] A. Boozer, Local equilibrium of nonrotating plasmas, Phys. Plasmas 9 (2002) 3762.

[13] S. Hirshman, J. Whitson, Steepest-descent moment method for three-dimensional magnetohydrodynamic equilibria, Phys. Fluids 26 (1983) 3553.

[14] R. Waltz, R. Miller, Ion temperature gradient turbulence simulations and plasma flux surface shape, Phys. Plasmas 6 (1999) 4265.

[15] J. Candy, A unified method for operator evaluation in local Grad-Shafranov plasma equilibria, Plasma Phys. Control. Fusion 51 (2009) 105009.

[16] J. Moré, B. Garbow, K. Hillstrom, User guide for MINPACK-1, Tech. Rep. ANL-80-74, Argonne National Laboratory, Argonne, IL, USA (Aug. 1980).